RSC Advances

ROYAL SOCIETY OF CHEMISTRY

www.rsc.org/advances

Journal Name

ARTICLE

Low Temperature Electrolysis for Iron Production via Conductive Colloidal Electrode

Qiang Wang, Yi Zhu, Qiuyang Wu, Eric Gratz, Yan Wang*

ABSTRACT: The iron and steel industry has a history of environmental consciousness, and efforts are continually made to reduce energy consumption and CO_2 emissions. However, the carbothermic process limits the further reduction of green house gas emissions, and only marginal improvements can be expected. Here, a novel and environmental friendly method about electrochemical reduction of Fe_2O_3 to produce Fe is introduced at low temperature of 110°C in alkaline solution. In the process, an electrical-ionic conductive colloidal electrode containing the electrochemically active species (Fe_2O_3 particles), the liquid electrolyte (NaOH solution), and a percolating electrical conductor (C network) has been successfully fabricated and utilized to produce Fe. The simultaneous percolation of electrons and ions effectively increases the area of the current collector, and enables the process to function at higher currents/rates. To enhance the faradic efficiency and energy efficiency in the electrolyzing process, Ti plate, which has low catalytic activity toward H_2 evolution reaction, was selected as current collector for cathode, and Pt foil which has high catalytic activity toward O_2 evolution reaction, was utilized as the current collector for anode. XRD results confirmed all Fe_2O_3 was reduced to Fe and Fe_3O_4. The research can potentially lead to Fe smelting by reducing an aqueous Fe_2O_3 colloidal electrode directly to Fe powder with no direct carbon emissions.

ARTICLE

Introduction

Fe is the most widely used metal, and currently nearly all crude Fe is produced by reducing Fe ores with coke in a blast furnace at a temperature of ~ 2000°C [1]. This carbothermic reduction process directly produces liquid metal, but it generates 2 metric tons of CO_2 per metric ton of crude Fe produced. [2] In addition to carbon emissions from the blast furnace, the iron and steel industry contributes greenhouse gas (GHG) in several ways, including coke production emissions, the use of carbonate flux during calcination, and emissions from the carbon electrodes in electric arc furnaces. [3]

The iron industry has a history of environmental consciousness, and efforts are continually made to reduce energy consumption and CO_2 emissions. [4] However, the carbothermic process limits the further reduction of GHG, and only marginal improvements can be expected. Therefore, radical, transformational technologies are required to achieve major improvement of drastic reductions of GHG emissions. In order to achieve this goal, many alternatives have been extensively studied to produce Fe with less/no direct carbon emissions. The details of the various approaches are presented below.

Sadoway et al. at MIT [5-8] have been studying molten oxide electrolysis (MOE) to produce liquid metal and O_2, which occurs by the decomposition of Fe_2O_3 dissolved in an appropriately designed solvent melt according to the reaction given by equation (1). With the use of an inert anode, MOE is theoretically capable of tonnage of metal production with O_2 as the only by-product; as a result, MOE produces no direct GHG emissions. However, the main challenge to MOE is finding an effective inert anode, due to the oxidation that occurs at high temperatures (~1500°C). Recently, they have made a significant improvement to overcome the oxidation of the anode, through the formation of an electrically conductive solid solution of chromium and aluminum oxides in the corundum structure [9].

$$4Fe^{3+} + 6O^{2-} \rightarrow 4Fe(l) + 3O_2(g) \qquad (1)$$

Sohn et al. at the University of Utah have been studying hydrogen flash smelting (HFS) to produce pure Fe. [10-21] In the process, H_2 is used to reduce magnetite Fe_3O_4 to Fe by gas-solid flash reduction at ~1200°C, and the molten Fe is collected. This technology allows bypassing the problematic pelletization/sintering and coke-making steps required in blast furnace iron-making [20]. However, currently hydrogen is still cost prohibitive as a reducing agent.

Low temperature electrolysis (LTE) for Fe production in alkaline solutions has been known for over half a century. [21-23] Recently, the interest in developing a new iron making process with low/zero GHG emission has led to the re-examination of LTE-based process. [24-27] In such a process, the reduction of Fe_2O_3 is carried out in a strong alkaline aqueous electrolyte (50 wt% $NaOH-H_2O$ at ~100°C), in which finely ground hematite Fe_2O_3, micrometer range particles are suspended, and some particles adhere to surface of electrode through diffusion, then reduced to Fe at the cathode. Only O_2 is produced at the anode, without direct GHG emissions.

Haarberg et al. deoxidate hematite with LTE, and high purity of Fe with six-twin crystal pyramid shape was obtained.[28] The cathode and anode reactions for LTE are shown in equations (2) and (3), respectively. Compared to the MOE and HFS processes, LTE process has a much lower operating temperature (~100 °C), which potentially leads to a simpler and less expensive process design.

Cathode: $Fe_2O_3(s) + 3H_2O + 6e^- \rightarrow 2Fe(s) + 6OH^-$ (2)

Anode: $6OH^- \rightarrow 3/2O_2(g) + 3H_2O + 6e^-$ (3)
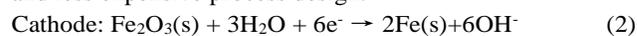
However, two reasons prevent LTE process from being adopted in commercial plants: (1) Fe_2O_3 particles adhering on surface of electrode is very limited, and the method is difficult to be scaled up. [24] (2) Since Fe_2O_3 has very poor electrical conductivity, the reduction of Fe_2O_3 pellet has very low reaction rate and energy efficiency.

In this study, a colloidal electrode was created, which contains the electrochemically active species (Fe_2O_3 particles), the liquid electrolyte (NaOH solution), and a 3D percolating electrical conductor (C network). The simultaneous percolation of electrons and ions effectively increase the area of the current collector, and enables the process to function at high currents rates.

Experimental

Preparation of colloidal electrode

To prepare a high electrical-ionic conductive colloid, a certain amount of C (Ketjen back, Akzo Nobel) and 39.4 g of sodium hydroxide (reagent grade, Amresco) were added into 48.1 g of DI water (Millipore DI water). The reactant Fe_2O_3 powder (diameter under 5μm, Sigma-Aldrich), and 0.9 g of sodium dodecylbenzenesulfonate (SBDS) (reagent grade, Aldrich), which helps to stabilize the dispersion of Fe_2O_3 powder, were added in the NaOH solution. Tube roller rolled the mixer for overnight, and was then stirred by homogenizer for 10 minutes before electrolysis was carried on.

Preparation of Fe_2O_3 ink electrode

50 mg Fe_2O_3 powder was ultrasonically dispersed into 5ml Nafion/ethanol solution (0.05wt% Nafion in ethanol) to form "ink" like suspension. 5μl "ink" was dropped onto a glass carbon electrode (diameter of glass carbon is 5mm), and dried. Then Fe_2O_3 particles, which is bonded together by Nafion, piled up on the surface of glass carbon to form a thin layer with thickness of 1μm.

Electrolysis of colloid

The electrolysis was conducted in a two-electrode electrolytic cell, as shown in Fig. S 1. The homogeneously mixed Fe_2O_3 colloid was coated on Ti plate (area 1.2 cm^2) and wrapped by a polyethylene separator. Here Ti plate was selected as current collect for cathode, as it has very low catalytic activity towards H_2 evolution reaction, which is shown in Fig. S 2. The detailed electrochemical behavior will be discussed in the following

paragraphs. The counter electrode is a platinum foil (area 3 cm^2) which has low overpotential toward O_2 evolution reaction and can increase the energy current efficiency. The electrodes were inserted into electrolyte which is 45wt% of NaOH solution, and the electrochemical cell was maintained at 110°C. The voltage between two electrodes was controlled by Potentiostat (EC-Lab, Biologic Science) at 1.7 V, which will be explained in the following paragraph. After being electrolyzed for 5 hours, electrodes were pulled out from electrolytic cell and the product was collected and washed with DI water and ethanol. Then the reduction product was dried in oven at 70^0C for 12 hours, and its component and surface topography was characterized by XRD, and SEM.

Cyclic Voltammetry test of Fe₂O₃ ink electrode in three-electrode cell

A three-electrode cell is utilized to determine the redox process of Fe_2O_3/Fe. The working electrode is Fe_2O_3 ink electrode with Hg/HgO as reference electrode, and the counter electrode is Pt wire electrode. CV was carried out in 20wt% NaOH solution in room temperature with the scan rate of 10mV/s.

Results and discussion

Conductivity of Colloidal electrode

In a short, the method about electrolyzing Fe_2O_3 suspension in alkaline solution can be summarized into three ways [24-27]. One is to disperse hematite particles in alkaline solution by continuous stirring, and the particles adhering to surface of electrode is reduced. Although the particles do not obey to simple diffusion, micrometer sized hematite particles would have a Stokes–Einstein diffusivity near 10^{-14} $m^2 \cdot s^{-1}$ in the alkaline electrolyte at 100 °C and the reaction rate and productivity are limited by the area of 2 dimensional electrod and the diffusion speed of particle in electrolyte. Fe_2O_3 particles need to diffuse to the electrode surface for the electrolysis occuring, which is shown in Fig. 1(a). The collision probability between hematite particles and electrode surface is also a bottle neck for the reaction rate. Additionally, the residence time about hematite particle adsorption on electrode surface may be short, and the particle was probably partly reduced. To understand the adsorption of hematite particle on surface of electrode, zeta potential of hematite was measured in electrolyte with different pH value and concentration of Na^+ by Siebentritt, and they found the zeta potential of hematite particle is neutral or slightly positive in strong alkaline. [29]

The second way is that a special electrolytic cell with rotating cathode or anode was designed. [26] These kinds of cells can indeed enhance the contact efficiency between cathode and hematite particles, and remove the produced gas phase rapidly, but the two rotating electrodes are subjected to appreciable ohmic losses.

The third way is pressing Fe_2O_3 particles into pellet, and metal
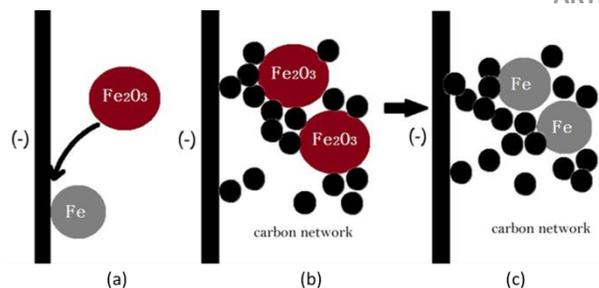
Figure 1. Schematic representation of Fe_2O_3 electrochemical reduction process in (a) Fe_2O_3 particles dispersing in alkaline solution, and in (b) & (c) an electrical-ionic conductive colloid.

wire is inserted into the pellet as current collector. The deficiency that electrical conductivity of Fe_2O_3 particle is poor limits the dimension of pellet can't be large.

In our approach, since the colloidal electrodes possess both electrically and ionically conductive properties, hematite particles don't need to diffuse from bulk solution to the surface of electrode for electrolyzing, and the conversion rate from Fe_2O_3 to Fe is not limited by the residence time of the particle adsorbed on electrode surface. The carbon network can conduct the electrons, which forms a 3D reaction network shown in Fig. 1(b)&(c). This will significantly increase the reaction area and reation rate. Here, SDBS was added into the colloid as the function of surfactant to stabilize the dispersion Fe_2O_3 in colloid. [27] The cathode, which Haarberg et al applied in electro-deoxidation of Fe_2O_3, also has 3D reaction interface. [30] However the colloid electrode in our experiment was adulterated with carbon and NaOH, therefore it can be easily reduced. Further more the colloid has the property of fluibility, which is demonstrated in Fig 2.

The effect of weight percentage of carbon on the electrical conductivity of colloid was systematically studied in our experiment, and adding carbon not only increases electrical conductivity of the colloid, but also increase its viscosity. As we know, the carbon particle dispersed in colloid attracts (Van der Waals force) and collides with each other when flowing, so increasing weight percentage of carbon inevitably increases the viscosity of colloid. Fig. 1 (b) and (c) sketch the microstructure of carbon network and the reduction mechanism of Fe_2O_3. The electrical conductance of colloid was measured with weight percentage of carbon from zero to 4wt% with the increment of 0.5wt%. The testing method is the following: the colloid is sandwiched between two steel cylindrical electrodes in a plastic cylinder. As the diameter of the electrodes fits the inner diameter of the cylinder well, the cross-sectional area (A) of the colloid is almost equal to the cross-sectional area of electrode, and the length of colloid (l) is the distance between two electrodes. Control the voltage between two electrodes by chronoamperometry technique at 0.1 V. For low voltage, the electrochemical reaction happened on the surface of electrode can be neglected, and the current (I) passed through colloid was almost electronic current. The electrical resistance (R) of colloid can be calculated by equation (4):

$$R = 0.1/I \qquad (4)$$

And its corresponding electrical conductivity (δ) can be calculated by equation (5):

$$\delta = R \cdot A / l \qquad (5)$$

The viscosity about the colloids with a series of weight percentage of carbon was test by rheometer (Bohlin DSR-F). From Fig. 2 (a), we can see both electrical conductivity and viscosity of colloids increase remarkably when the weight percentage of carbon was up to 4%.
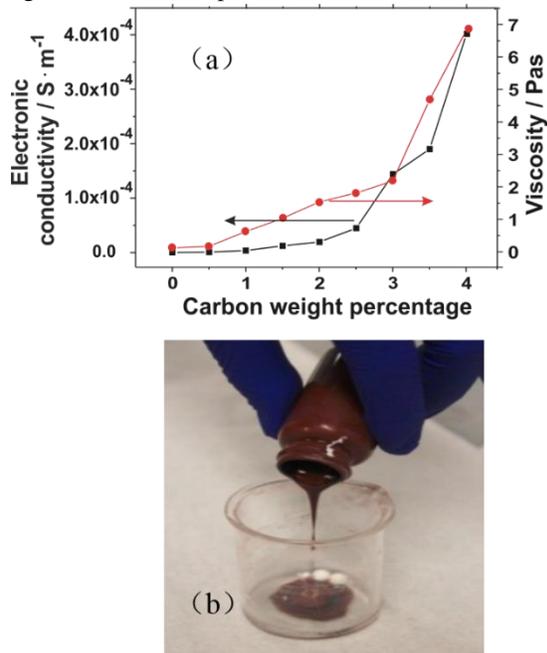
Figure 2. (a) The dependence of electrical conductivity and viscosity of colloid on weigh percentage of carbon (Ketjen black). (b) The fluidity of colloid with 2.5wt% of carbon.

The colloid should possess some kind of fluidity, which can be utilized in practical production of Fe in a flowing device. To walk a fine line between conductivity and viscosity, the percentage of carbon is optimized to 2.5wt%, and the electrical conductivity of colloid is about 2×10^{-4} S/cm. According to the electrical conductivity measure, we estimated that the colloid with the thickness of 2 mm on the surface of Ti current collector (the dimension of Ti is 1.5cm $\times$ 2cm) has the resistance of 300 Ω, the total Fe_2O_3 can be reduced through electrochemical method in our experiment, which will be proved with our experiment later on. This benefited from the special structure of the colloid electrode. During the reduction processing, Fe_2O_3 in close proximity to Ti current collector is reduced to Fe firstly, and good conductivity of Fe increased electrical conductivity of the colloid, then Fe_2O_3 far away from current collector can be more easily reduced. The colloid with good fluidity is demonstrated in Fig. 2 (b). Good fluidity will allow us to design "flow electrolysis" in the later research, which is similar to flow batteries.

The redox process of Fe_2O_3 ink electrode

The anodic oxidation of iron in alkaline solution was wildly investigated, because it related to cycling performance in Fe/Ni, Fe/air batteries and corrosion of iron. [32-34] For the electrochemical oxidation of iron, it is generally accepted that three or four anodic cyclic voltammetric peaks, and various species, such as $Fe(OH)_2$, Fe_3O_4, γ-Fe_2O_3, δ-FeOOH, α-FeOOH, and β-FeOOH were reported to explain those peaks. [34,35] For the cathodic reduction of Fe_2O_3 in alkaline solution, there are probably two mechanisms to explain the reduction process. One is hematite dissolves in alkaline solution, and dissolved iron ion is reduced, according to Eq. (6) - (8).

$$2Fe_2O_3 + 3H_2O + 2OH^- \rightarrow Fe(OH)_4^- \qquad (6)$$
$$Fe(OH)_4^- + e^- \rightarrow Fe(OH)_3^- + OH^- \qquad (7)$$
$$Fe(OH)_3^- + 2e^- \rightarrow Fe^0 + 3OH^- \qquad (8)$$
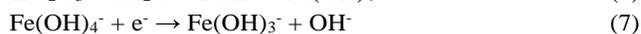
However, as the dissolution of Fe_2O_3 in 50wt% NaOH solution is 2×10^{-3} M, and the dissolution rate is very slow, this mechanism can't be the main process of Fe_2O_3 reduction.

Another mechanism is reducing Fe_2O_3 solid particles directly through the steps described by Eq. (9) – (12), which correspond to three or four cathodic peaks during cyclic voltammetric testing. Some of peaks may not be observed under certain experimental conditions: [35,36]

$$3Fe_2O_3 + 2H^+ + 2e^- \rightarrow 2Fe_3O_4 + H_2$$
$$E_o = 0.221-0.0591pH \qquad (9)$$
$$Fe_2O_3 + 2H^+ + 2e^- \rightarrow 2FeO + H_2O$$
$$E_o = -0.057-0.0591pH \qquad (10)$$
$$FeO + 2H^+ + 2e^- \rightarrow Fe + H_2O$$
$$E_o = -0.047-0.0591pH \qquad (11)$$
$$Fe_3O_4 + 8H^+ + 8e^- \rightarrow 3Fe + 4H_2O$$
$$E_o = -0.085-0.0591pH \qquad (12)$$
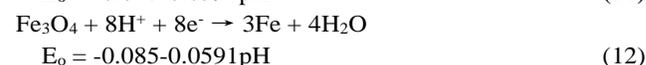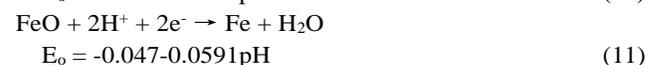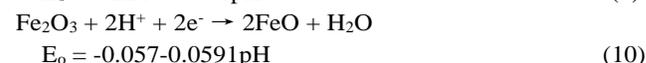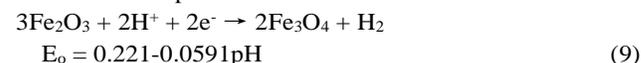
Caldas et al. reported triangular sweep voltagmmetry curve of porous iron electrode in alkaline solution, and only the cathodic peak corresponding to the reduction of Fe(Ⅲ) to Fe(Ⅱ) was observed. [37] Other cathodic peaks were not visible, as they were superimposed by dramatically increasing reduction current related to H_2 evolution reaction.

As its value of equilibrium potential is between the potential of equation (9) and potential of equation (12), H_2 evolution reaction is the competing reaction during the process of electrolyzing Fe_2O_3, and it decreases the faradic efficiency of electrolyzing Fe_2O_3.

$$2H^+ + 2e^- \rightarrow H_2$$
$$E_o = -0.0591pH \qquad (13)$$

In our experiment, we use Fe_2O_3 ink electrode with 1 μm thickness of Fe_2O_3 particle layer on the surface of glass carbon, which can eliminate the poor conductivity of Fe_2O_3 particle as much as possible, for the CV test in the scan rate of 10mV/s, and the result is shown in Fig. 3. In the first cycle, peak I, which is supposed to be the reduction from Fe_2O_3 to Fe, is the main cathodic peak with the peak potential of -1.06V (vs. Hg/HgO). However before peak I, Fe_2O_3 is already reduced from 0V (vs. Hg/HgO) slowly, and this part of reduction process may be related to some $Fe^{Ⅲ}$ reduced to $Fe^{Ⅱ}$. After -1.16V (vs. Hg/HgO), there is a dramatically increasing cathodic current, which is related to H_2 revolution. After first cycle, there are two cathodic peak peaks Ⅱ and Ⅲ, and peak Ⅱ decreases with peak Ⅲ increases. We suppose that after the first cycle, Fe_2O_3 was converted to $Fe(OH)_3$, which has different electrochemical property and structure with Fe_2O_3, and the reduction of $Fe(OH)_3$ relates to two main steps: $Fe(OH)_3 \rightarrow Fe(OH)_2$, $Fe(OH)_2 \rightarrow Fe$. During the potential

scaning from low to high potential, Fe is gradually oxidized to $Fe(OH)_2$ and $Fe(OH)_3$. However, the transformation from $Fe(OH)_2$ to $Fe(OH)_3$ is very hard. [38] When the potential reach to 0.6V (vs. Hg/HgO), more and more $Fe(OH)_2$ accumulates, and less and less $Fe(OH)_3$ produces when cycling carries on.
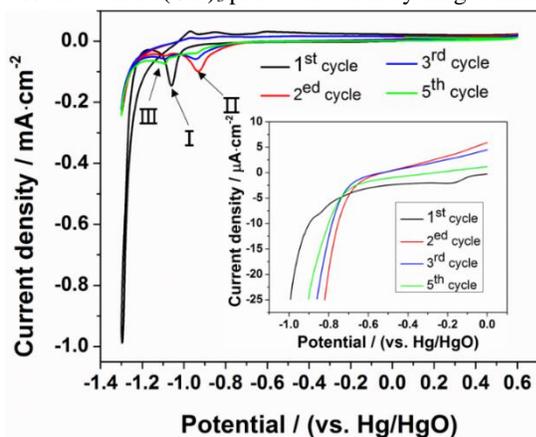
Figure 3. The CV of Fe_2O_3 ink electrode in 20wt% NaOH solution with scan rate of 10mV/s.

This coincides with the phenomenon that peak Ⅱ decreases with peak Ⅲ increases. After 10 cycle, peak Ⅱ disappeared and only peak Ⅲ left. The CV test also demonstrates the reduction of Fe_2O_3 is accompanyed by H_2 evolution.

Eletrochemical reduction of Fe_2O_3 colloid

In the two-electrodes electrolyzing experiment, different metals were chosen as the cathode current collector to determine the catalytic activity toward H_2 evolution reaction. As Fig. S 2 showed, Ti electrode has the lowest reduction current of 1 mA, and it is good for enhancing the faradic efficiency toward reducing Fe_2O_3. During Fe_2O_3 reduction on cathode, oxidation reaction happened simultaneously on anode. As equation (2) expressed, OH^- was oxidized to O_2 on anode. For its high catalytic activity toward O_2 revolution reaction, Pt was selected as anode which is helpful for increasing the electric energy efficiency.

In the electrolyzing process, 0.8 g Fe_2O_3 colloid was coated on the surface of Ti electrode, and was electrochemically reduced with chronoamperometry technique at 1.7 V, which is a optimized value to balance Fe_2O_3 reduction and H_2 revolution. We tried the voltage of 1.3V, 1.4V, 1.5V, 1.6 V and 1.7 V to electrolyze the Fe_2O_3 colloid, and found the cathodic current is very small when the value of voltage is less than 1.7 V, which is shown in Fig. S 3. In the diagram of electrolyzing Fe_2O_3 colloid, four distinct kinetic regimes in the current transit were observed in Fig. 4 (a): (1) a rapid current increased in the first half an hour; (2) a slow current increased in the later an hour; (3) a slow current decrease in the later an hours; (4) and a relative stable current in the last 2 hours. At the first half an hour, electrochemical reaction was likely established on the Fe_2O_3/electrolyte interface, so the current increased very rapidly. After half an hour, some Fe_2O_3 particles were reduced
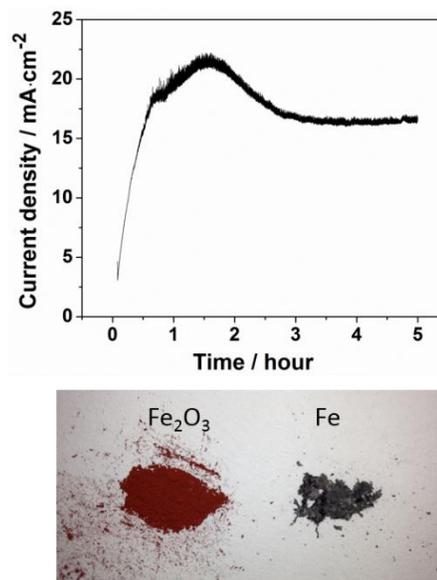
Figure 4. (a) Electrochemical reduction of Fe_2O_3. With chronoamperometry technique adopted, and the voltage between two electrodes was controlled at 1.7 V; (b) The reactant of Fe_2O_3 and production of Fe.

to Fe gradually, and H_2 revolution reaction happened on the surface of Fe particles accompanying Fe_2O_3 reduction, which is verified by CV test in Fig. 3. Two parallel reactions are responsible for gradually increased current. When the reduction processed for 1.5 hours, most of Fe_2O_3 was reduced to Fe, and the H_2 revolution reaction became the main reaction. This is responsible for the slow current decay. After 3 hours reduction, only H_2 evolved on the surface of Fe particles. Therefore, the integration of the peak area in Fig. 4 (a) is the amount of charge which not only contains the charge of reduction of Fe_2O_3, but also includes the charge of H_2 evolution. The electrolysis was operated for 5 hours to ensure that all Fe_2O_3 was reduced, and then the reduced product was dried in oven at 70°C for several hours. The color of the powder changed from its original red to grey, as Fig. 4 (b) shown.

XRD and SEM were adopted to characterize the reduction product. Fe_2O_3 was completely reduced as only Fe and Fe_3O_4 can be detected by XRD shown in Fig. 5. Even though the charge is enough to reduce all the Fe_2O_3 into Fe based on faradic law and the mass of Fe_2O_3, productivity of pure Fe in our experiment is low. The main reason is that part of the charge is comsumed for H_2 revolution reaction, and this is vertified by Fray [40], as when Na_2O is added, which can make H_2 evolution hard, more Fe_2O_3 will be reduced to Fe. Secondly, during the reduction of Fe_2O_3, some H_2 was trapped in the colloid and then made the electronic conductivity lower. Thirdly, forming Fe_3O_4 with Fe and H_2O is a spontaneous and thermodynamically favorable reaction, as equation (14) demonstrates:

$$3\ Fe\ (s) + 4\ H_2O\ (g) \rightarrow Fe_3O_4\ (s) + 4\ H_2\ (g) \qquad (14)$$
$$\triangle G = -101.03\ kJ$$
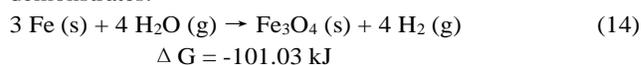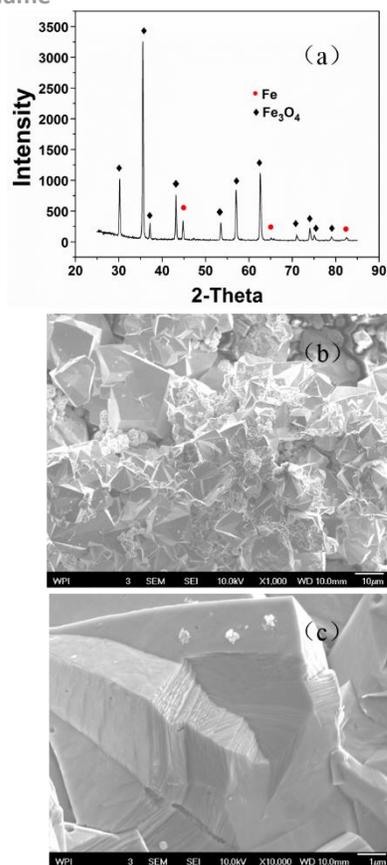
Figure 5. (a) X-ray diffraction of electrochemical reduction product of Fe_2O_3; (b) & (c) SEM test about the product with different magnification.

As the fresh Fe produced by electrochemical reduction is highly active, and it can react with H_2O spontaneously to form a Fe_3O_4 layer on the surface of Fe, after the electrolysis stopped, but Fe_3O_4 layer can stop the reaction going on. We put commercial pure iron powder (200 mesh, sigma) into alkaline solution in 100 °C for 30min, and found about 1wt% of Fe converted to Fe_2O_3. Fourthly, as reported by Casellato, [36] Fe_3O_4 reduced from Fe_2O_3 is almost totally resistant to on-going electrochemical reduction, and the reduction of Fe_3O_4 is a very slow reaction. SEM demonstrates the diameter of particle produced by electrochemical reduction is micrometer and it has morphology of laminated structure shown in Fig. 5 (b).

Conclusions

A uniformly dispersed Fe_2O_3 colloid, which has high ionic conductivity and electronic conductivity, was prepared. In our experiment, Ti plate, which has low catalystic activity toward H_2 evolution reaction, was utilized as cathode current collector, and Pt electrode, which has high catalystic activity toward O_2 evolution reaction, was utilized as anode in the electrolysis process, in order to enhance the electric energy efficiency and faradic efficiency. As its by-product is only O_2 and the electrolysis carried on in low temperature, the method introduced here is environmental friendly and high electric

energy utilization. XRD confirms that Fe_2O_3 is reduced to Fe_3O_4 and Fe. To further enhance the conversion rate from Fe_2O_3 to Fe and the faradic efficiency, some additives which can enhance the electrical conductivity of Fe_2O_3 and suppress the HER on iron and carbon particle surface will be added into electrolyte in the future research.

Journal Name

ARTICLE

Notes and references

*Y. Wang, E-mail: yanwang@wpi.edu, Tel: 508-831-5453, Fax: 508-831-5178

.

† Footnotes should appear here. These might include comments relevant to but not central to the matter under discussion, limited experimental and spectral data, and crystallographic data.

Electronic Supplementary Information (ESI) available: [details of any supplementary information available should be included here]. See DOI: 10.1039/b000000x/

1. U.S. Geological Survey, Iron and Steel, Mineral yearbook 2007, Advance Release, U.S Department of Interior, April 2009; p 37.5.

2. http://www.iea.org/publications/freepublications/publication/tracking_emissions.pdf.

3. http://www.epa.gov/climateleadership/documents/resources/ironsteel.pdf.

4. M.Yellishetty, P. G. Ranjitha, *Resour Conserv. Recy*. 2010. **54**, 1084.

5. D. H. Wang, A. J. Gmitter, and D. R. Sadoway, *J. Electrochem. Soc.* 2011. **158**, E51.

6. D. R. Sadoway, *J. Mater. Res.* 1995. **10**, 487.

7. H. Kim, J. Paramore, A. Allanore, and D. R. Sadoway, *J. Electrochem. Soc.* 2011. **158**, E101.

8. H. Kim, J. Paramore, A. Allanore, and D. R. Sadoway, *ECS Transactions*, 2010. **33**, 219.

9. A. Allanore,; L. Yin, and D. R. Sadoway, *Nature*, 2013. **497**, 4.

10. H. K. Pinegar, M. S. Moats, and H. Y. Sohn, *Ironmak. Steelmak*. 2012. **39**, 398.

11. H. K. Pinegar, M. S. Moats, and H. Y. Sohn, *Ironmak. Steelmak*. 2013. **40**, 32.

12. H. K. Pinegar, M. S. Moats, and H. Y. Sohn, *Ironmak. Steelmak.* 2013. **40**, 44.

13. M. E. Choi, and H.Y. Sohn, *Ironmak. Steelmak*. 2010. **40**, 81.

14. M. Y. Mohassab‐Ahmed, H. Y. Sohn, and H. G. Kim, *Ind. Eng. Chem. Res.* 2012. **51**, 7028.

15. M. Y. Mohassab‐Ahmed, H. Y. Sohn, and H. G. Kim, *Ind. Eng. Chem. Res.* 2012. **51**, 3639.

16. H. K. Pinegar, M. S. Moats, and H.Y. Sohn, *Steel Res. Int.* 2011. **82**, 951.

17. H. Y. Sohn, and M. E. Choi, *J. Iron Steel Res. Int.* 2009. **16**, 1283.

18. H. Y. Sohn, et al.; *Energy Technology Perspectives: Conservation, Carbon Dioxide Reduction and Production from Alternative Sources*, 2009. 93.

19. I. Sohn, and D. J. Min, *Steel Res. Int.* 2012. **83**, 611.

20. H. T. Wang, and H.Y. Sohn, *Metall. Mater. Trans. B* 2013. **44**, 133.

21. J. A. M. LeDuc, R. E. Loftfield, and L. E. Vaaler, *J. Electrochem. Soc.* 1959. **106**, 659.

22. S. J. Lloyd, *Trans. Am. Electrochem. Soc.* 1929. **55**, 305.

23. Offray; French Pat. FR 228753, 1974.

24. A. Allanore, J. Feng, H. Lavelaine, and K. Ogle, *J. Electrochem. Soc.* 2010. **157**, 24.

25. A. Allanore, H. Lavelaine, J. P. Birat, G. Valentin, F. Lapicque, *J. Appl. Electrochem.* 2010. **40**, 1957.

26. A. Allanore, H. Lavelaine, G. Valentin, J. P. Birat, and F. Lapicque, *J. Electrochem. Soc.* 2008. **155**, 125.

27. A. Allanore, H. Lavelaine, G. Valentin, J. P. Birat, F. Lapicque, M. D. Clark, and S. Subramanian, *Electrochim. Acta* 2010. **55**, 4007.

28. G. M. Haarberg, B. Yuan, *ECS Transactions*, 2014. **58**, 19.

29. M. Siebentritt, P. Volovitch, K. Ogle, and G. Lefevre, Colloids Surf., A, 2014. **440**, 197.

30. R. Krishnamoorti, *J. Colloid Interface Sci.* 2011, **354**, 144.

31. A. Inoishi, Y. W. Ju, S. Ida, and T. Ishihara, *J. Power Sources* 2013, **229**, 12.

32. A. Inoishi, S. Ida, S. Uratani, T. Okano, T. Ishihara, *PCCP* 2012, **14**, 12818.

33. C. A. C. Souzaa, I. A. Carlosb, M. Lopes, *J. Power Sources* 2004, **132**, 288.

34. P. Periasamy, B. R. Babu, S.V., Iyer, *J. Power Sources* 1996, **58**, 35.

35. H. Zhang, and S. M., Park, *J. Electrochem. Soc.* 1994, **141**, 718.

36. Pourbaix, M., Atlas of electrochemical equilibria in aqueous solutions, National association of corrosion engineers, 1974, 307.

37. U. Casellato, N. Comisso, G. Mengoli, *Electrochim. Acta* 2006. **515**, 669.

38. S. Valeska, and M. D. Thomas, *J. Electrochem. Soc.* 1999. **146**, 4061.

39. A. Bewick, M. Kalaji, and G. Larramona, J. Electroanal. Chem., 1991. **318**, 207.

40. A. Cox, and D. J. Fray, *Ironmak. Steelmak*. 2008. **35**, 561.